

# QCD equation of state in a virial expansion

S. Mattiello and W. Cassing

*Institute for Theoretical Physics, University of Gießen, Germany*

We describe recent three-flavor QCD lattice data for the pressure, speed of sound and interaction measure at nonzero temperature and vanishing chemical potential within a virial expansion. For the deconfined phase we use a phenomenological model which includes non-perturbative effects from dimension two gluon condensates that reproduce the free energy of quenched QCD very well. The hadronic phase is parameterized by a generalized resonance-gas model. Furthermore, we extend this approach to finite quark densities introducing an explicit  $\mu$ -dependence of the interaction. We calculate pressure, quark-number density, entropy and energy density and compare to results of lattice calculations. We, additionally, investigate the structure of the phase diagram by calculating the isobaric and isentropic lines as well as the critical endpoint in the  $(T, \mu_q)$ -plane.

PACS numbers: 12.38.Mh, 25.75.Nq, 21.65.Qr, 12.38Aw

## I. INTRODUCTION

The exploration of the phase structure of quantum chromodynamics (QCD) for the whole density-temperature plane is a challenging task for the standard model. Lattice Monte Carlo simulations have revealed several exciting results over the past decade [1, 2, 3, 4, 5, 6, 7, 8]. At finite densities, modeling of QCD has added substantially to our understanding of its rich phase structure [9, 10, 11, 12, 13, 14, 15, 16, 17, 18, 19, 20, 21]. In the last years heavy-ion collision experiments focus on the investigation the quark-gluon plasma (QGP). Early concepts of the QGP were guided by the assumption of a weakly interacting systems of partons because the entropy density  $s$  and the energy density  $\varepsilon$  calculated from lattice QCD were close to the Stefan Boltzmann (SB) limit for a relativistic noninteracting system. However, recent observations at the Relativistic Heavy Ion Collider (RHIC) indicated that the QGP created in ultrarelativistic Au + Au collision was interacting more strongly than hadronic matter [22, 23, 24, 25, 26, 27, 28]. Because of these experimental facts the noticeable deviation ( $\approx 10 - 15\%$ ) became more important.

In the hadronic phase of QCD the partition function of a hadron resonance-gas yields a satisfactory description of lattice results on bulk thermodynamic observables in the low temperature region for  $\mu_q = 0$  [29] and in the general case at finite densities, i.e.  $\mu_q \neq 0$  [30]. In this context the investigation of the interaction between the partons in the deconfined phase plays a crucial role to understand the properties of the QGP. The dynamical quasiparticle picture is one important way to relax the approximation of the QGP as an ideal gas [17, 18, 31, 32] of massive but noninteracting degrees of freedom. Alternatively, the phase structure can be investigated in the finite width model (FWM) by analyzing its isobaric partition given by a generalization of statistical ensembles with fluctuating extensive quantities [33, 34]. Another possibility is to use a generalized formalism to calculate the corrections to a single-particle partition function starting from an interaction potential.

In this work we use the latter formalism, which is a generalized version of the classical virial expansion, to calculate the partition function with an interaction potential extracted from lattice calculations.

The paper is organized as follows: In Section II we introduce the virial expansion for vanishing quark chemical potential  $\mu_q$ . In Section III we motivate our model for the hadronic as well as for the deconfined phase and in Section IV we show the results of the virial expansion within our model. We extend in Section V the virial expansion to finite densities and again compare our results with lattice calculations. Furthermore, we explicitly evaluate the confinement-deconfinement phase transition and the isobaric and isentropic lines. The conclusions in Section VI finalize this work.

## II. VIRIAL EXPANSION AT $\mu_q = 0$

The main quantity to establish thermodynamical properties of QCD is the partition function  $Z(T, V)$ . In this Section we restrict ourselves to the case of vanishing chemical potential  $\mu_q$ , i.e. vanishing baryon number. The partition function then is obtained as

$$Z(T, V) = \text{Tr} [e^{-\beta H}], \quad (1)$$

where  $H$  is the Hamiltonian of the system and  $\beta = 1/T$  is the inverse temperature. For particles with spin-isospin degeneracy factor  $d$  the logarithm of the partition function reads

$$\ln Z = d \int_V d^3\mathbf{r} \int d^3\mathbf{p} \eta \log \left( 1 + \eta e^{-\beta H(\mathbf{r}, \mathbf{p})} \right), \quad (2)$$

where  $\eta = -1$  for bosons and  $\eta = 1$  for fermions.

In the case of an interaction free system, the Hamiltonian  $H(\mathbf{r}, \mathbf{p})$  is given by the kinetic energy  $E_k$  and therefore depends on  $p = |\mathbf{p}|$  only. For massless particles one has (with  $\hbar = c = 1$ )  $H(p) = p$  and can calculate the

partition function for bosons as well as for fermions,

$$\ln Z_B = d_B V \frac{\pi^2}{90\beta^3} \equiv V \ln Z_B^{(0)} \quad (3)$$

$$\ln Z_F = d_F V \frac{7\pi^2}{720\beta^3} \equiv V \ln Z_F^{(0)}. \quad (4)$$

Accordingly, the boson and the fermion partition functions are connected by

$$d_B \ln Z_F^{(0)} = \frac{7}{8} d_F \ln Z_B^{(0)}. \quad (5)$$

For non-interacting particles with mass  $m$  the Hamiltonian is given by  $H(p) = \sqrt{p^2 + m^2}$  and the partition function can be expressed in terms of the Bessel function  $K_2$ .

From the partition function all thermodynamic quantities can be derived: pressure, energy density, entropy, interaction measure and velocity of sound. Using the free massless partition function this leads to the well-known Stefan Boltzmann limit.

To relax the dependence on the size of the system we divide the partition function by the volume  $V$  and all calculated quantities become densities. In general we are not able to calculate exactly the partition function except by numerical diagonalization of the many-body Hamiltonian. To incorporate the effect of interactions we start with the classical virial expansion. To this aim we consider the  $N$ -body Hamiltonian defined by

$$H_1(\mathbf{r}_1, \mathbf{p}_1) = E_k(p_1) \quad (6)$$

$$H_2(\mathbf{r}_1, \mathbf{r}_2, \mathbf{p}_1, \mathbf{p}_2) = E_k(p_1) + E_k(p_2) + W_{12} \quad (7)$$

$$H_3(\mathbf{r}_1, \mathbf{r}_2, \mathbf{r}_3, \mathbf{p}_1, \mathbf{p}_2, \mathbf{p}_3) = E_k(p_1) + E_k(p_2) + E_k(p_3) + W_{123} \quad (8)$$

...

In classical physics the Bose as well the Fermi distributions in Eq. (2) merge to the Boltzmann distribution and the logarithm in the integrand drops. Then, we can separate the kinetic and the interaction term in the partition function. To recover the quantum statistics we perform a minimal substitution by replacing the integral over the momentum by the integral for the free case, which leads to the exact Stefan Boltzmann limit. The definition

$$\zeta = \ln Z^{(0)}, \quad (9)$$

where we suppressed for simplicity the indices for fermion and bosons, leads to an expansion of the partition function in powers of  $\zeta$ , i.e.

$$Z = \sum_{\nu=0}^{\infty} \frac{b_\nu}{\nu!} \zeta^\nu. \quad (10)$$

We consider only the first two terms of this expansion: then the coefficients are given by

$$b_1 = 1 \quad (11)$$

$$b_2 = \int_V d^3\mathbf{r} \left( e^{-\beta W_{12}(r)} - 1 \right). \quad (12)$$

The pressure reads

$$P = T \ln Z = T \sum_{\nu=1}^{\infty} \frac{b_\nu}{\nu!} \zeta^\nu, \quad (13)$$

and can be directly expressed in terms of the particle density  $\rho$ . We obtain for the first terms of the expansion

$$P = T\rho \left( 1 - \frac{b_2}{2}\rho + \dots \right). \quad (14)$$

The other quantities can be calculated from the pressure or the partition function using the thermodynamic relations:

$$\varepsilon = -\frac{\partial \ln Z}{\partial \beta} \quad (15)$$

$$s = \frac{\partial P}{\partial T}. \quad (16)$$

$$c_s^2 = \frac{dP}{d\varepsilon} = \varepsilon \frac{dP/\varepsilon}{d\varepsilon} + \frac{P}{\varepsilon}. \quad (17)$$

### III. THE MODEL

The application of the virial expansion formalism to investigate the properties of the hadronic and partonic matter requires the calculation of the single-particle partition function for the degrees of freedom and of the corrections given by the residual interaction between the 'constituents'. For the confined phase the degrees of freedom are the hadrons while in the QGP phase they are the quarks/antiquarks as well as the gluons.

The analysis of thermodynamic properties of the hadronic phase has demonstrated that a good description is achieved using a phenomenological resonance-gas model taking into account all mesonic and baryonic resonances with masses up to 1.8 GeV and 2.0 GeV, respectively. This amounts to 1026 resonances that truly are experimental parameters of the model [8]. In this case the residual interaction may be neglected. However, to reduce the number of the experimental parameters for the description of the low temperature region of QCD we explicitly write the partition function of the resonance-gas in the Boltzmann limit as [35]

$$\ln Z(V, T) = \sum_{i=1} \frac{VT m_i^2}{2\pi^2} \rho(m_i) K_2\left(\frac{m_i}{T}\right), \quad (18)$$

where the sum begins with the stable ground state  $m_0$  and includes the resonances  $m_i, i = 1, 2, \dots$  with weights  $\rho(m_i)$  relative to  $m_0$ . To specify  $\rho(m_i)$  we employ the Hagedorn hypothesis [36, 37] of an exponential growth of the number of hadronic resonances with mass. The formula for the asymptotic dependence of the density of hadronic states on mass  $m$  is given by

$$\rho(m) = f(m) \exp\{m/T_H\}, \quad (19)$$

where  $f(m)$  denotes a slowly varying function and  $T_H$  is the Hagedorn temperature estimated to be in the range of 180 – 210 MeV. We choose the form

$$f(m) = am^{-\alpha}, \quad \alpha = 3/2 \quad (20)$$

defined for  $m_0 \geq 140$  MeV taking into account that the pions are the hadronic states with the lowest mass. We now replace the sum in the resonance-gas partition function (18) by an integral and insert the exponentially growing mass spectrum (19) with the choice of  $f(m)$  (20),

$$\ln Z(V, T) = \frac{aVT}{2\pi^2} \int_{m_0}^{\infty} dm \sqrt{m} \exp\{m/T_H\} K_2\left(\frac{m}{T}\right). \quad (21)$$

In the limit of low temperatures, i.e.  $z = m/T \gg 1$ , the Bessel function can be approximated by,

$$K_2(z) = \sqrt{\frac{\pi}{2z}} \exp\{-z\}, \quad (22)$$

and the integral in the resonance-gas partition function (21) can be solved analytically. This gives

$$\ln Z(V, T) = aV \left(\frac{T}{2\pi}\right)^{3/2} \frac{\exp\{-m_0 b\}}{b}, \quad b = \frac{1}{T} - \frac{1}{T_H}, \quad (23)$$

and leads to a good description of the thermodynamical variables.

To perform a realistic investigation of the properties of the QGP we have to determine a realistic effective interaction between the partons in the deconfined phase. The starting point for this aim is provided by lattice calculations for the quark-antiquark free-energy. There are many parametrizations of this quantity and several discussions about the role as effective potentials (or alternatively as the internal energy) [38]. We adopt the parametrization of the free energy given by Megias et al. in Ref. [39]. This phenomenological model includes non-perturbative effects from dimension two gluon condensates. This one-gluon exchange model, introduced in Ref. [40] for the description of the Polyakov loop, allows for a good parametrization of the singlet heavy quark-antiquark free energy lattice data in gluon-dynamics. The connection between dimension two gluon condensates and QGP-properties has been confirmed by recent fits of the interaction measure in gluon-dynamics in terms of the condensate [42, 43].

The expression for the free energy in this model is given by

$$F_1(r, T) = V_1(r, T) + F_1(\infty, T), \quad (24)$$

where  $F_1(\infty, T)$  is the singlet free energy at infinite separation and  $V_1$  is the effective potential for the deconfined phase. We use

$$V_1(r, T) = - \left( \frac{\pi}{12} \frac{1}{r} + \frac{C_2}{2N_c T} \right) e^{-M(T)r}, \quad (25)$$

where  $C_2$  is the non-perturbative dimension two condensate and  $M(T)$  a Debye mass estimated as

$$M(T) = \sqrt{N_c/3 + N_f/6} gT = \tilde{g}T. \quad (26)$$

The parameters have been determined in Ref. [39] from a fit to the lattice data of the Polyakov loop in gluon-dynamics, i.e.  $N_f = 0$ ,

$$C_2 = (0.9 \text{ GeV})^2 \quad (27)$$

$$\tilde{g}_{\text{PL}} = 1.26. \quad (28)$$

In our calculations we will consider light quarks instead of heavy quarks (with infinite mass) and hence expect deviations from the previous values (27) and (28). Accordingly, we consider  $\tilde{g}$  as a free parameter that we may fix in comparison with  $N_f = 3$  lattice calculations [8] for the pressure (calculated for  $N_\tau = 6$ ). These lattice calculations imply a critical temperature  $T_c \approx 196$  MeV for the deconfinement phase transition.

#### IV. RESULTS

Using the one-gluon exchange potential we can directly calculate the pressure from Eq. (13) for the QGP. To calculate the second virial coefficient  $b_2$  we linearize the exponential function in Eq.(12). For the hadronic phase we calculate the pressure from the partition function using Eq. (13). By comparing the lattice results of the pressure  $P/T^4$  as a function of the temperature for the deconfined phase (given by  $T \geq T_c = 196$  MeV) with our results we find a good agreement with  $\tilde{g}$  in the range  $1.25 \leq \tilde{g} \leq 1.35$ . Note that these values for  $\tilde{g}$  are comparable with the result from the fit of the Polyakov loop, i.e.  $\tilde{g}_{\text{PL}} = 1.26$ . Our fit in the deconfined region yields  $\tilde{g} = 1.30$  and we can fix the value of the Hagedorn temperature  $T_H$  and the constant  $a$  to obtain a continuous function for all temperatures  $T > 0$ . This leads to  $T_H = 205$  MeV and  $a = 9.17 \text{ MeV}^{1/2}$ .

In Fig. 1 we show the lattice results of the scaled pressure  $P/T^4$  as a function of the temperature expressed in units of the critical temperature  $T_c = 196$  MeV and the pressure from the virial expansion with the parameters fixed above.

Since all thermodynamic quantities are connected by known relations (cf. (14)-(17)) we expect that the lattice data for all quantities are compatible with the results from our model, too. To confirm this we show in Fig. 2 the entropy density  $s$  divided by  $T^3$  as a function of the temperature expressed in units of the critical temperature using Eq.(16).

Another interesting quantity is the square of the velocity of sound  $c_s^2$  defined by Eq.(17). In the high temperature limit as well as in the transition region, where the derivative  $d(P/\varepsilon)/d\varepsilon$  vanishes,  $c_s^2$  is given by  $p/\varepsilon$ . The results of our model for this quantity (as a function of the fourth root of the energy density) are shown in Fig. 3 for  $T_c = 196$  MeV (solid) in comparison with the lattice data

(blue squares). They show (as expected) a good agreement with the lattice data for  $\varepsilon^{1/4}/(\text{GeV}/\text{fm}^3)^{1/4} \geq 1.3$  which is equivalent to  $T \geq T_c$ . The dashed line is the parametrization in the high temperature region with the simple *Ansatz* [41]

$$\frac{P}{\varepsilon} = \frac{1}{3} \left( C - \frac{A}{1 + B\varepsilon \text{ fm}^3/\text{GeV}} \right), \quad (29)$$

that provides a good fit to the data in the interval  $1.3 \leq \varepsilon^{1/4}/(\text{GeV}/\text{fm}^3)^{1/4} \leq 6$  with  $C = 0.964(5)$ ,  $A = 1.16(6)$  and  $B = 0.26(3)$  [8]. The current resolution and accuracy of lattice calculations for the hadronic region clearly are not yet sufficient to allow for a detailed comparison with any model calculation. The dotted line in Fig. 3 indicates the exact square of the sound velocity. The difference between this quantity and the ratio  $P/\varepsilon$  indicates the deviation from a linear dependence between pressure and energy density valid at high temperature. This linear behavior is confirmed in Fig. 3 for high energy densities, where  $c_s$  as well as  $P/\varepsilon$  show the Stefan Boltzmann limit of  $1/3$ .

In the framework of the one-gluon exchange model the interaction measure  $W = \varepsilon - 3P$  plays an important role and was recently investigated in detail in Refs. [42, 43]. From the fit of  $W$  in the deconfined region in gluon-dynamics the value of the dimension two gluon condensate has been calculated in an independent way without considering the Polyakov loop. However, the results of the two approaches show only little deviation when using  $1.26 \leq \tilde{g} \leq 1.45$ . The calculation of the interaction measure using the virial expansion starting with a model motivated by the fit to the Polyakov loop may directly indicate a dynamical connection between the two methods. For this reason we show in Fig. 4 the interaction measure divided by the fourth power of the temperature  $W/T^4$  as a function of the temperature expressed in units

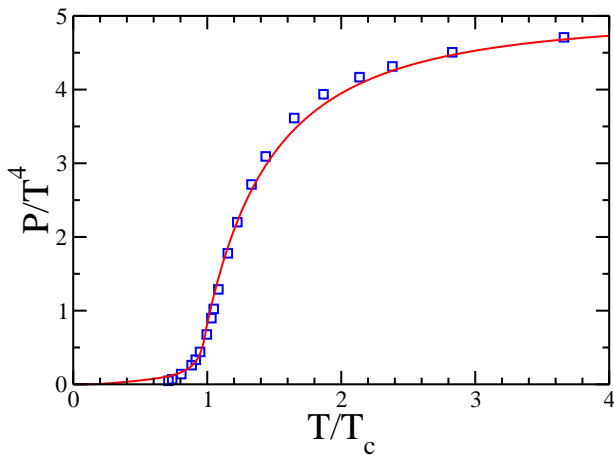


FIG. 1: (Color online) Pressure  $P$  as a function of the temperature divided by  $T^4$  for  $\tilde{g} = 1.30$ ,  $T_H = 205$  MeV and  $a = 9.17 \text{ MeV}^{1/2}$  in comparison to the lattice data from Ref. [8].

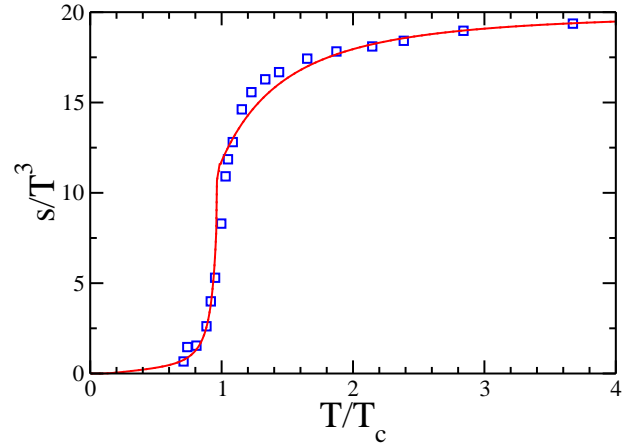


FIG. 2: (Color online) Entropy density  $s$  as a function of the temperature divided by  $T^3$  for  $\tilde{g} = 1.30$ ,  $T_H = 205$  MeV and  $a = 9.17 \text{ MeV}^{1/2}$  in comparison to the lattice data from Ref. [8].

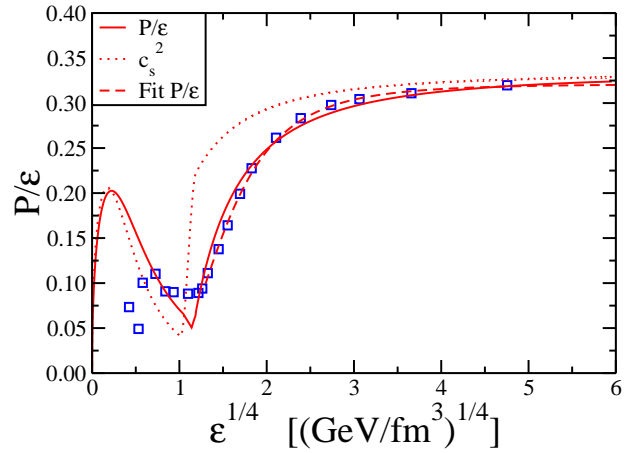


FIG. 3: (Color online) Ratio  $P/\varepsilon$  as a function of the fourth root of the energy density for the critical temperature  $T_c = 196$  MeV in comparison to the lattice data from Ref. [8].

of the critical temperature  $T_c = 196$  MeV, where the expected agreement with the lattice data (blue squares) is observed.

## V. FINITE QUARK CHEMICAL POTENTIAL

The extension of the virial expansion to non-vanishing quark chemical potentials  $\mu_q$  requires an explicit dependence of the interaction on the quark chemical potential. Since the interaction is primarily determined by the Debye mass  $M$ , we may generalize the interaction for non-vanishing  $\mu_q$  by introducing an explicit dependence for the Debye mass only, i.e.  $M(T) \rightarrow M(T, \mu_q)$ . We parameterize this dependence by

$$M(T, \mu_q) = M^{(0)}(T) F\left(\frac{\mu_q}{T}\right), \quad (30)$$

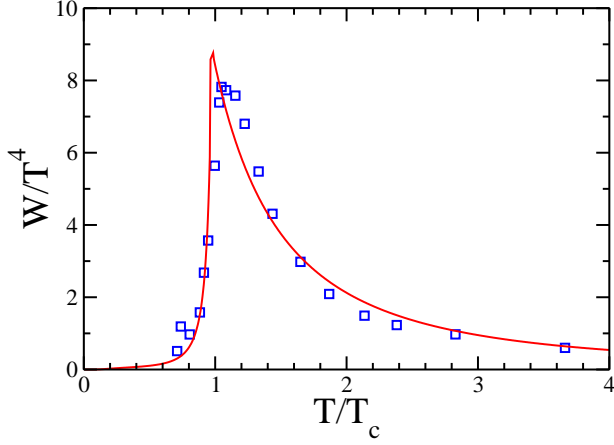


FIG. 4: (Color online) The interaction measure  $W$  as a function of the temperature divided by  $T^4$  for  $\tilde{g} = 1.30$ ,  $T_H = 205$  MeV and  $a = 9.17$  MeV $^{1/2}$  in comparison to the lattice data from Ref. [8].

where  $M^{(0)}(T) = M(T, \mu_q = 0)$  denotes the Debye mass at vanishing chemical potential and  $F$  describes the modification at finite density. This assumption is equivalent to introduce a  $\mu_q$ -dependence of the coupling  $\tilde{g}$  (in our model),

$$\tilde{g} \longrightarrow \tilde{g}^* \left( \frac{\mu_q}{T} \right) = \tilde{g} F \left( \frac{\mu_q}{T} \right). \quad (31)$$

Furthermore, perturbation theory suggests that the leading order contribution to the correction is given by [44]

$$F_{\text{PT}} \left( \frac{\mu_q}{T} \right) = \sqrt{1 + \frac{3N_f}{(2N_c + N_f)\pi^2} \left( \frac{\mu_q}{T} \right)^2}. \quad (32)$$

For our calculations we generalize this expression as follows,

$$F \left( \frac{\mu_q}{T} \right) = A \left( \frac{\mu_q}{T} \right) F_{\text{PT}} \left( \frac{\mu_q}{T} \right), \quad (33)$$

with

$$A \left( \frac{\mu_q}{T} \right) = 1 + \frac{1}{\pi^2} \left( \frac{\mu_q}{T} \right)^2, \quad (34)$$

where the value of the coefficient  $\pi^{-2}$  is consistent for  $N_f = 3$  with Ref. [45]. For the hadronic phase we use an effective modification of the constant  $a$  given formally in Eq.(31). Choosing in this case the perturbative correction we obtain

$$a \longrightarrow a^* \left( \frac{\mu_B}{T} \right) = a F_{\text{PT}} \left( \frac{\mu_B}{T} \right), \quad (35)$$

where  $\mu_B = 3\mu_q$  indicates the baryonic chemical potential.

At nonzero chemical potential, typical quantities of interest that become accessible from lattice calculations are the (scaled) pressure difference defined as

$$\frac{\Delta P(T, \mu_q)}{T^4} = \frac{P(T, \mu_q) - P(T, \mu_q = 0)}{T^4} \quad (36)$$

and the scaled quark number density given by

$$\frac{n_q(T, \mu_q)}{T^3} = \frac{1}{T^3} \frac{\partial P(T, \mu_q)}{\partial \mu_q} = \frac{1}{T^4} \frac{\partial P(T, \mu_q)}{\partial (\mu_q/T)}. \quad (37)$$

Since for  $\mu_q \neq 0$  direct Monte Carlo calculations are not applicable, higher order derivatives of the pressure with respect to  $\mu_q/T$  at  $m_{u_q} = 0$  are calculated and then the pressure is estimated using a Taylor expansion,

$$\frac{P(T, \mu_q)}{T^4} = \frac{\ln Z(T, \mu_q)}{T^3} = \sum_{n=0}^{\infty} c_n(T) \left( \frac{\mu_q}{T} \right)^n, \quad (38)$$

where the expansion coefficients are given in terms of derivatives of  $\ln Z(T, \mu_q)$ , i.e.

$$c_n(T) = \frac{1}{n! T^3} \frac{\partial^n \ln Z}{\partial (\mu_q/T)^n}. \quad (39)$$

The series (38) is even in  $\mu_q/T$  which reflects the invariance of  $Z(T, \mu_q)$  under exchange of particles and antiparticles. The coefficients  $c_2$  and  $c_4$  have been calculated for two-flavor QCD in Ref. [4]; an extension to the sixth order is given in Ref. [5]. To evaluate the pressure and the other thermodynamics quantities within the virial expansion we can formally use the expansion given in Eq. (13), where the expansion parameter  $\zeta$  now depends on the quark chemical potential, i.e.  $\zeta \longrightarrow \tilde{\zeta}(\mu_q)$ . Using the Taylor expansion of the pressure in the Stefan Boltzmann limit we can explicitly give this  $\mu_q$ -dependence of  $\zeta$ . In this case the coefficients are well known as

$$c_2^{\text{SB}} = \frac{N_f}{2}, \quad c_4^{\text{SB}} = \frac{c_2}{(2\pi)^2}, \quad c_n^{\text{SB}} = 0 \quad \text{for } n \geq 6. \quad (40)$$

Now we can rewrite the generalized expansion parameter as

$$\tilde{\zeta}(\mu_q) = \zeta + c_2^{\text{SB}} T^2 \mu_q^2 + c_4^{\text{SB}} \frac{\mu_q^4}{T}. \quad (41)$$

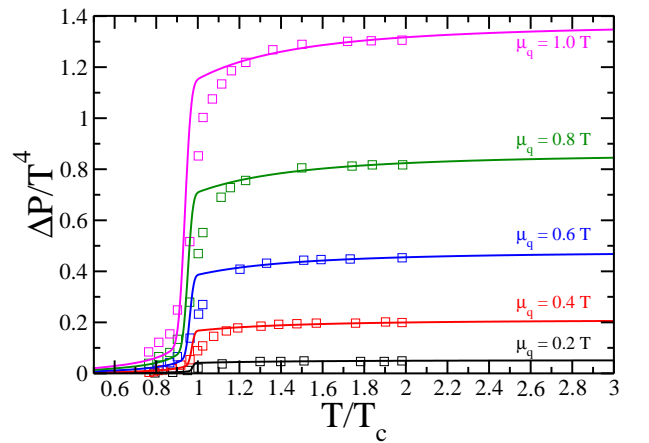


FIG. 5: (Color online) Scaled pressure difference as a function of the temperature for different values of  $\mu_q/T$  compared to lattice calculations taken from Ref. [4].

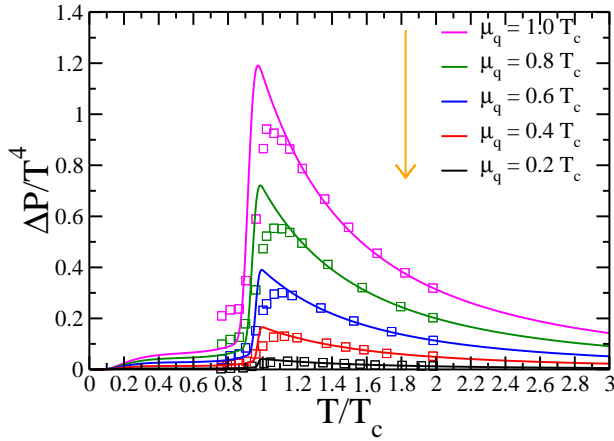


FIG. 6: (Color online) Scaled pressure difference as a function of the temperature for different values of  $\mu_q$  compared to lattice calculations taken from Ref. [4].

The results for the scaled pressure difference as a function of the temperature (expressed in units of the critical temperature  $T_c = 196$  MeV) are shown in Fig. 5 for various values of  $\mu_q/T$ . The data points are the lattice results for  $N_f = 2$  from Ref. [4] scaled to  $N_f = 3$ . Lattice results for three-flavor QCD are not yet available and partial data for  $N_f = 2 + 1$  are preliminary only [48, 49]. The agreement between our results and the lattice simulations is quite satisfactory. In the region around  $T_c$  there is a deviation from the scaled lattice points.

This is better visible in an analogue representation of the results in Fig. 6, where the scaled pressure difference is shown as a function of the temperature expressed in units of the critical temperature  $T_c = 196$  MeV for various values of the quark chemical potential  $\mu_q$ . We note an overestimation of the pressure difference around the critical temperature. This can be understood by considering the possible errors of the scaling procedure as well

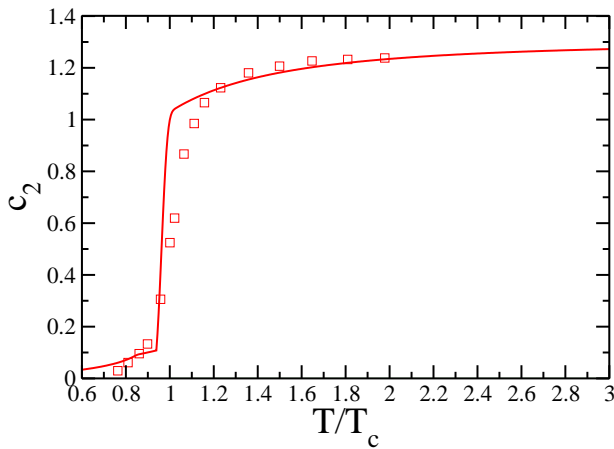


FIG. 7: (Color online) Coefficient  $c_2(T)$  of the Taylor expansion for the pressure as function of  $T/T_c$  compared to lattice calculations taken from Ref. [4].

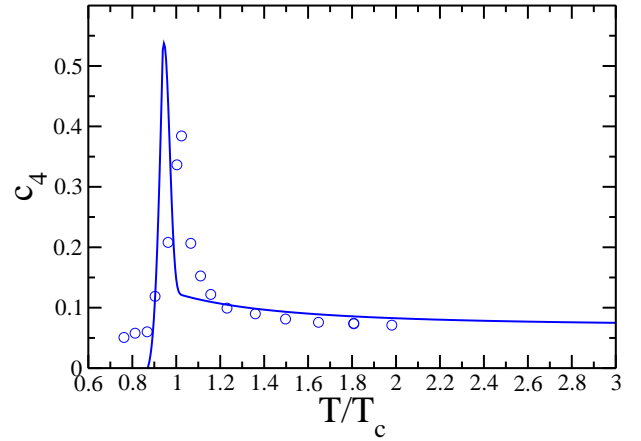


FIG. 8: (Color online) Coefficient  $c_4(T)$  of the Taylor expansion for the pressure as a function of  $T/T_c$  compared to lattice calculations taken from Ref. [4].

as by the errors given by the (truncated) Taylor expansion itself.

We can now calculate the coefficients  $c_2(T)$  and  $c_4(T)$  of the Taylor expansion for the pressure by the least-square method. The comparison with the scaled lattice results from Ref. [4], shown in Fig. 8, is quite satisfactory. Analogue comparisons with quasiparticle models are given in Refs. [46, 47]. Although these coefficients allow to directly evaluate the scaled quark number density, we prefer to use the definition given in Eq.(37) because the Taylor sum is only an expansion up to the fourth order and its validity for strongly interacting system is not so clear (cf. Ref. [50]). Our results for  $n_q/T^3$  as a function of the temperature (in units of the critical temperature  $T_c = 196$  MeV) are shown in Fig. 9 for various values of the quark chemical potential  $\mu_q$ . Also in this case, the comparison between our virial calculation and the corresponding (scaled) lattice data shows a slight overestimation close to  $T_c$ .

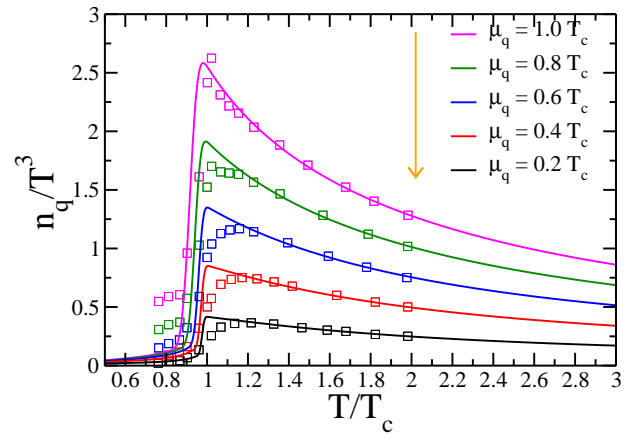


FIG. 9: (Color online) Scaled quark number density as a function of the temperature for different values of  $\mu_q$  compared to lattice calculations taken from Ref. [4].

Using the results for the pressure and the entropy density (from Eq.(16)) we can directly investigate the structure of the QCD phase diagram in the  $\mu_q - T$  plane. Starting from the point at zero chemical potential, i.e.  $(0, T_c)$ , we calculate the isobaric ( $P = \text{const.}$ ) as well as isentropic ( $s = \text{const.}$ ) lines in the phase diagram which are shown in Fig 10 by the solid and dot-dashed lines, respectively. The resulting isentropic temperature at the phase boundary is practically constant up  $\mu_q \approx 200$  MeV, whereas the isobaric temperature at the phase boundary (solid line) drops with increasing chemical potential. This behavior quantitatively agrees with the critical line (dashed) from lattice calculations within the reweighting method from Ref. [51]. The observation that the critical phase transition is a line at constant pressure is also confirmed by lattice simulations in Ref. [51]. The dotted line in Fig. 10 shows the region  $\mu \leq T$ , where the lattice results are expected to be valid. For comparison we display also the hadron chemical freeze-out line (dash-dash-dot) using the parametrization given in Ref. [52]. Note that the hadron freeze-out - determined experimentally from hadron ratios - clearly occurs in the hadronic phase for all  $\mu_q$  with a sizeable gap in temperature relative to the phase transition line.

Furthermore, a detailed investigation of the isobaric line leads to a first estimate for the critical endpoint  $(\mu_E, T_E)$ , where the crossover in the low density region changes to a first order phase transition. Following Ref. [53] the curvature of the crossover - separating the QGP and the hadronic phase - is given by

$$T/T_c = 1 - \tilde{C}\mu_q^2/T_c^2. \quad (42)$$

To evaluate the critical endpoint we perform a corresponding parametrization of our calculated isobaric line. This only works if  $\chi^2 \leq 1$ , i.e. a maximum of the chemical potential exists which satisfies this condition; the latter value defines the chemical potential of the endpoint. From our analysis we obtain  $\mu_E = 117 \pm 5$ , which is in agreement with the results of the lattice calculation  $\mu_E^{(Lattice)} = 120 \pm 10$  from Ref. [53]. The corresponding critical point  $(\mu_E, T_E) = (117, 190)$  MeV is shown as a star in Fig 10.

We recall that the main aim of this paper is to evaluate the QCD equation of state in terms of physically measurable quantities. Following Ref. [4] we calculate the equation of state  $\Delta(p/T^4)$  vs  $(n_q/T^3)^2$  for different temperatures. The results are shown in Fig. 11, where the yellow region is delimited by the low- $T$  SB (upper boundary) and by the high- $T$  SB limit (lower boundary). For temperatures near- but below -  $T_c$  the equation of state shows a form resembling the low- $T$  SB limit

$$\Delta P = \frac{1}{4}(\pi^2/N_f)^{1/3}n_q^4. \quad (43)$$

As  $T$  increases though the critical temperature, the EoS changes from this functional dependence to the stiffer

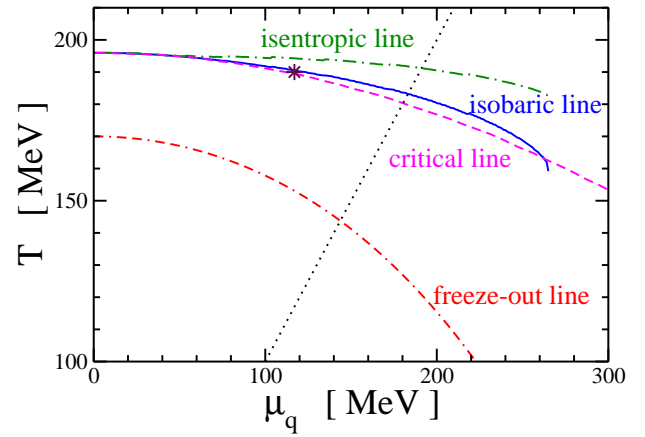


FIG. 10: (Color online) Overview of the QCD phase diagram with isobaric (solid) and isentropic lines (dash-dot) in comparison to the phase transition line (dashed) estimated in Ref. [51]. Also shown is the hadron chemical freeze-out line (dot-dash-dashed) in the parametrization given in Ref. [52]. The dotted line ( $T = \mu_q$ ) demonstrates the expected range of validity for the lQCD calculations.

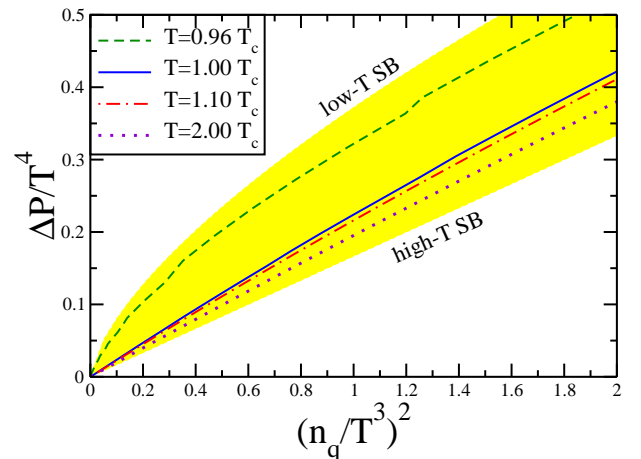


FIG. 11: (Color online) Equation of state  $\Delta(p/T^4)$  vs.  $(n_q/T^3)^2$  for various temperatures. The continuum Stefan Boltzmann forms for low and high  $T$  (given by (43) and (44)) are also shown as functions of  $T/T_c$ .

form of the high- $T$  SB limit given by

$$\Delta P = \frac{1}{2N_f}n_q^2. \quad (44)$$

The quadratic coefficient depends smoothly on the temperature and therefore shows a sizeable deviation from the exact Stefan Boltzmann limit also for  $T = T_c$ .

## VI. CONCLUSIONS

We have performed an investigation of QCD thermodynamic quantities within a virial expansion approach.

While hadronic matter is described by a generalized resonance-gas model, we fix the interaction in the QGP phase by lattice calculations for the heavy quark free energy. We adopt a phenomenological model which includes non-perturbative effects from dimension two gluon condensates that describe the free energy of quenched QCD very well at vanishing chemical potential. Explicit expressions for the partition function and the pressure in the deconfined phase are derived. Our results for  $\mu_q = 0$  and  $N_f = 3$  for pressure, entropy density, speed of sound and interaction measure at nonzero temperature compare well with three-flavor QCD lattice calculations with almost physical masses from Ref. [8]. We find that a coupling parameter  $\tilde{g} = 1.30$  provides a good agreement for all quantities. Note that this choice is close to the value determined in Ref. [39] from a fit to lattice data for the Polyakov loop in gluon-dynamics, i.e.  $\tilde{g}_{PL} = 1.26$ . The difference in the coupling parameters most likely is due to the different quark masses employed.

Furthermore, we have extended this approach to finite densities introducing an explicit  $\mu$ -dependence of the interaction (via the Debye mass following perturbation theory). This allows to calculate the thermodynamic quantities of interest such as pressure and quark-number density etc. also at finite  $\mu_q$ ; the results again compare well with lattice calculations scaled from  $N_f = 2$  to  $N_f = 3$  with minimal deviations at the critical temperature  $T_c$ . These differences are most visible in the pressure, become smaller for the scaled quark number density and lead to the open question about the validity of the Taylor expansion and its thermodynamic consistency.

Additionally, we have investigated the structure of the phase diagram also in the region inaccessible to lattice

calculations, i.e.  $\mu_q \geq T$ . We have calculated the isentropic and specially the isobaric line, which agrees remarkably well with the cross over transition evaluated by lattice calculations with the reweighting method. The direct knowledge of the partition function allows to calculate the equation of state of the quark gluon plasma which also reproduces very well the predictions of the lattice calculations. The EoS clearly shows two decisive properties of the QCD phase diagram: *i)* There is an unequivocal transition from the hadronic matter to deconfined matter as is evident from the change of the functional form of the equation state from the typical Stefan Boltzmann behavior for low to high temperatures. *ii)* The QGP is a strongly correlated system and sensitively differs from the ideal gas limit. Also at  $T = 2T_c$  there is a remarkable deviation of the EoS of the QGP from the Stefan Boltzmann limit which is a clear signal of surviving correlations in the deconfined phase.

Our equation of state has been dynamically calculated with a particular form of the interaction. Using the same interaction in molecular dynamical calculations we may systematically investigate relevant properties of the QGP such as the pair correlation function  $g(r)$ , the plasma parameter  $\Gamma$ , the structure factor  $S(q)$  or the shear viscosity  $\eta$ . Further interesting applications in this context (cf. Refs. [54, 55]) are relativistic molecular dynamic simulations, where the phenomenological quark-quark interaction used here can be implemented as well as the QCD equation of state. This will allow to study partonic systems also out of equilibrium.

*Acknowledgements:* Work supported by the Deutsche Forschungsgemeinschaft (DFG).

- 
- [1] M. J. Tannenbaum, Int. J. Mod. Phys. E **17**, 771 (2008).
  - [2] Z. Fodor, S. D. Katz and K. K. Szabo, Phys. Lett. B **568**, 73 (2003).
  - [3] Z. Fodor and S. D. Katz, JHEP **0203**, 014 (2002).
  - [4] C. R. Allton, S. Ejiri, S. J. Hands, O. Kaczmarek, F. Karsch, E. Laermann and C. Schmidt, Phys. Rev. D **68**, 014507 (2003).
  - [5] C. R. Allton *et al.*, Phys. Rev. D **71**, 054508 (2005).
  - [6] M. D'Elia and M. P. Lombardo, Phys. Rev. D **67**, 014505 (2003).
  - [7] M. D'Elia and M. P. Lombardo, Phys. Rev. D **70**, 074509 (2004).
  - [8] M. Cheng *et al.*, Phys. Rev. D **77**, 014511 (2008).
  - [9] M. G. Alford, K. Rajagopal and F. Wilczek, Phys. Lett. B **422**, 247 (1998).
  - [10] M. G. Alford, K. Rajagopal and F. Wilczek, Nucl. Phys. B **537**, 443 (1999).
  - [11] R. Rapp, T. Schäfer, E. V. Shuryak and M. Velkovsky, Phys. Rev. Lett. **81**, 53 (1998).
  - [12] K. Rajagopal and F. Wilczek, Shifman, M. (ed.): At the frontier of particle physics, vol. 3\* 2061, hep-ph/0011333.
  - [13] S. P. Klevansky, Rev. Mod. Phys. **64**, 649 (1992).
  - [14] M. Bluhm, B. Kämpfer and G. Soff, Phys. Lett. B **620**, 131 (2005).
  - [15] M. Bluhm, B. Kämpfer, R. Schulze, D. Seipt and U. Heinz, Phys. Rev. C **76**, 034901 (2007).
  - [16] C. Ratti, M. A. Thaler and W. Weise, Phys. Rev. D **73**, 014019 (2006).
  - [17] W. Cassing, Nucl. Phys. A **791**, 365 (2007).
  - [18] W. Cassing, Nucl. Phys. A **795**, 70 (2007).
  - [19] W. Cassing, Eur. Phys. J. ST **168**, 3 (2009).
  - [20] S. Mattiello, Few Body Syst. **34**, 119 (2004).
  - [21] S. Strauss, S. Mattiello and M. Beyer, arXiv:0903.5209 [hep-ph].
  - [22] M. Gyulassy and L. McLerran, Nucl. Phys. A **750**, 30 (2005).
  - [23] P. Jacobs and X. N. Wang, Prog. Part. Nucl. Phys. **54**, 443 (2005).
  - [24] H. Stöcker, Nucl. Phys. A **750**, 121 (2005).
  - [25] K. Adcox *et al.* [PHENIX Collaboration], Nucl. Phys. A **757**, 184 (2005).
  - [26] E. V. Shuryak, Nucl. Phys. A **750**, 64 (2005).
  - [27] U. W. Heinz, AIP Conf. Proc. **739**, 163 (2005).
  - [28] H. Song and U. W. Heinz, Phys. Lett. B **658**, 279 (2008).
  - [29] F. Karsch, K. Redlich and A. Tawfik, Eur. Phys. J. C **29**, 549 (2003).



- [30] F. Karsch, K. Redlich and A. Tawfik, Phys. Lett. B **571**, 67 (2003).
- [31] A. Peshier, Phys. Rev. D **70**, 034016 (2004).
- [32] A. Peshier and W. Cassing, Phys. Rev. Lett. **94**, 172301 (2005).
- [33] K. A. Bugaev, Phys. Atom. Nucl. **71**, 1585 (2008).
- [34] K. A. Bugaev, V. K. Petrov and G. M. Zinovjev, Europhys. Lett. **85**, 22002 (2009).
- [35] P. Blanchard, S. Fortunato and H. Satz, Eur. Phys. J. C **34**, 361 (2004).
- [36] R. Hagedorn, Nuovo Cim. Suppl. **3**, 147 (1965).
- [37] W. Broniowski, W. Florkowski and L. Y. Glozman, Phys. Rev. D **70**, 117503 (2004).
- [38] J. Liao and E. Shuryak, J. Phys. G **35**, 104058 (2008).
- [39] E. Megias, E. Ruiz Arriola and L. L. Salcedo, Phys. Rev. D **75**, 105019 (2007).
- [40] E. Megias, E. Ruiz Arriola and L. L. Salcedo, JHEP **0601**, 073 (2006).
- [41] S. Ejiri, F. Karsch, E. Laermann and C. Schmidt, Phys. Rev. D **73**, 054506 (2006).
- [42] E. Megias, E. R. Arriola and L. L. Salcedo, arXiv:0809.2044 [hep-ph].
- [43] E. Megias, E. Ruiz Arriola and L. L. Salcedo, arXiv:0805.4579 [hep-ph].
- [44] S. Ejiri *et al.*, Nucl. Phys. A **774**, 837 (2006).
- [45] A. Peshier, J. Phys. G **31**, S371 (2005).
- [46] M. Bluhm, B. Kämpfer and G. Soff, J. Phys. G **31**, S1151 (2005).
- [47] M. Bluhm and B. Kämpfer, Phys. Rev. D **77**, 034004 (2008).
- [48] P. Hegde, F. Karsch and C. Schmidt, arXiv:0810.0290 [hep-lat].
- [49] F. Karsch [RBC Collaboration and HotQCD Collaboration], J. Phys. G **35**, 104096 (2008).
- [50] M. Buballa, A. G. Grunfeld, A. E. Radzhabov and D. Scheffler, arXiv:0811.4543 [hep-ph].
- [51] C. R. Allton *et al.*, Phys. Rev. D **66**, 074507 (2002).
- [52] F. Karsch, J. Phys. Conf. Ser. **46**, 122 (2006).
- [53] Z. Fodor and S. D. Katz, JHEP **0404**, 050 (2004).
- [54] S. Mrowczynski and M. H. Thoma, Ann. Rev. Nucl. Part. Sci. **57**, 61 (2007).
- [55] B. A. Gelman, E. V. Shuryak and I. Zahed, Phys. Rev. C **74**, 044908 (2006).